

Electronic Supplementary Information (ESI)

Sequential multi-molecule delivery using vortex-assisted electroporation

Hoyoung Yun and Soojung Claire Hur*

The Rowland Institute at Harvard University, Cambridge MA, USA

*To whom the correspondence should be addressed: hur@rowland.harvard.edu

List of Supplementary Movie

Supplementary Movie 1. Sequential delivery of two inherently membrane impermeable molecules (YOYO[®]-1 and PI) into metastatic breast cancer cell lines (MDA-MB-231)

List of Supplementary Figures

ESI Figure 1. Target cell isolation mechanism and evolution of trapped cells' size distribution

ESI Figure 2. Schematic of the computer-assisted pneumatic flow control system

ESI Figure 3. Rapid solution exchange performance evaluation

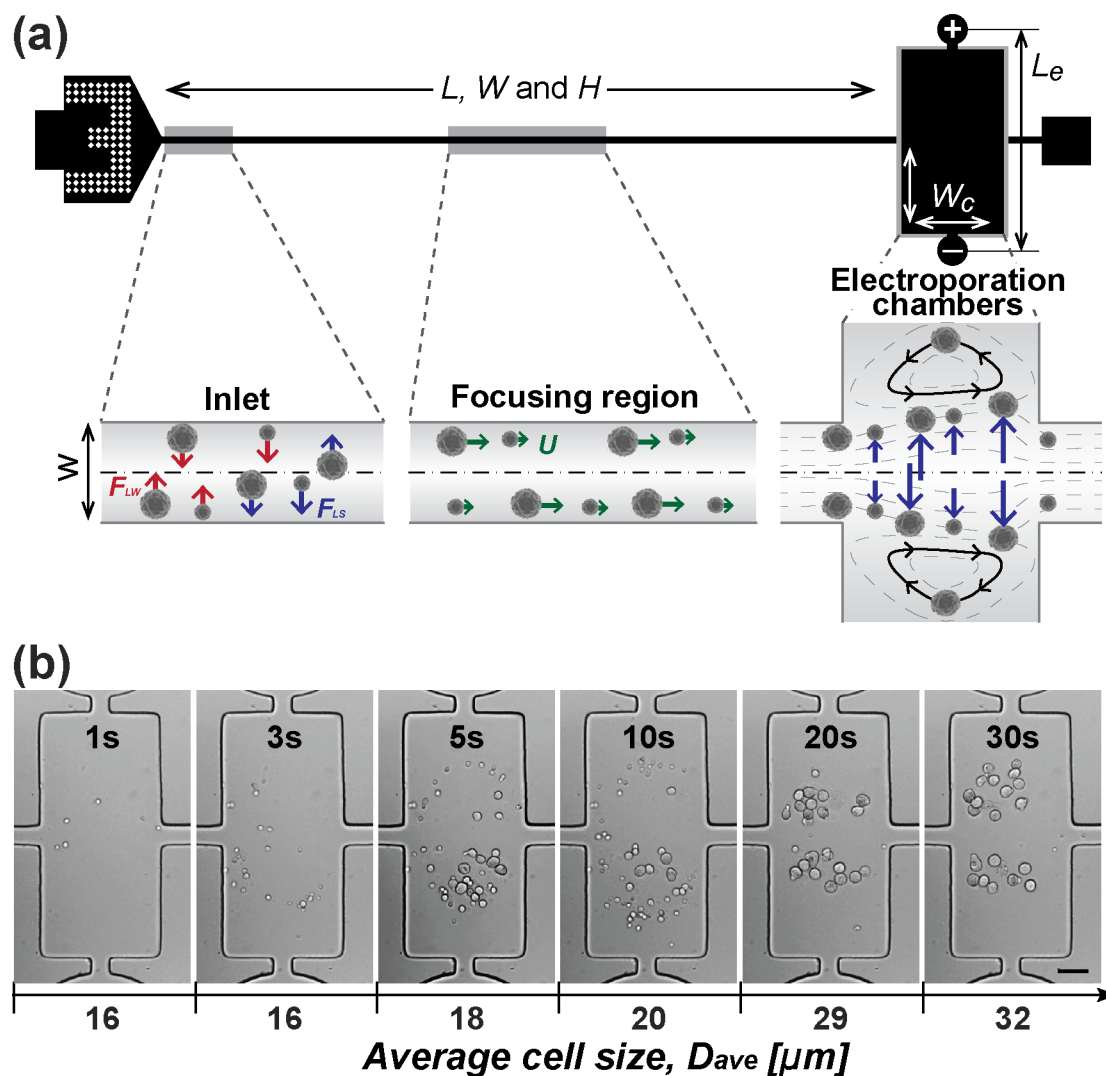
ESI Figure 4. Numerically simulated electric field distribution across the electroporation chamber under the tested conditions

ESI Figure 5. Size and quality verification of tested plasmids

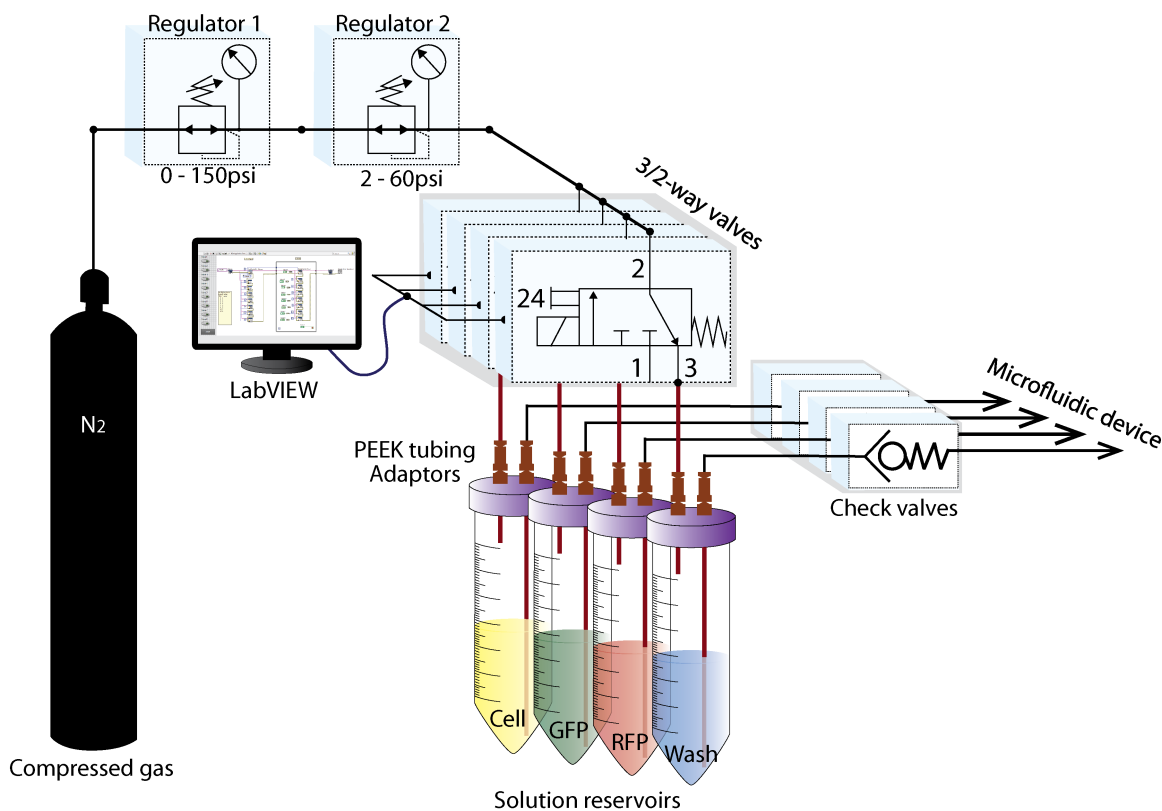
ESI Figure 6. Demonstration of precise dosage controllability on hard-to-transfect K562 cells

ESI Figure 7. Static electroporation without the size-based pre-selection

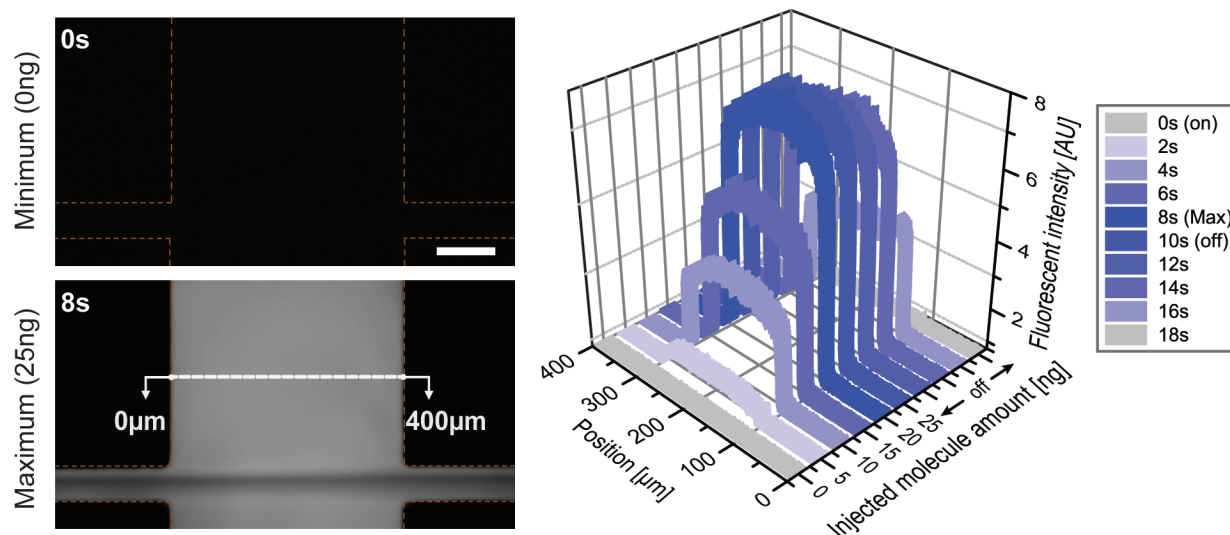
ESI Figure 8. Multigene transfection of MDA-MB-231 using the cuvette-type electroporation



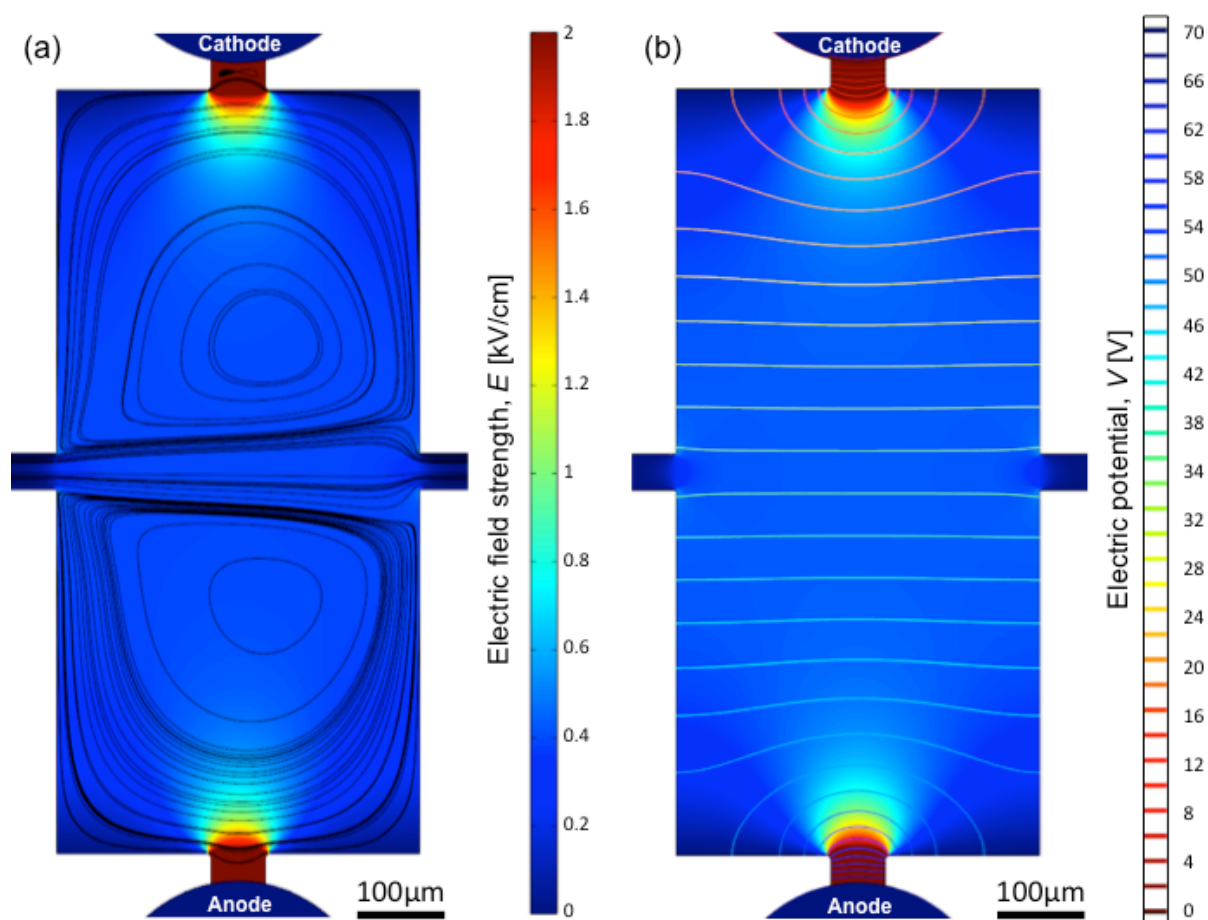
ESI Figure 1. (a) Device design and cell trapping principle. The device consists of the inlet region, the focusing region ($L = 4.5 \text{ cm}$, $W = 40 \mu\text{m}$, and $H = 60 \mu\text{m}$), the electroporation chambers ($W_c = 400 \mu\text{m}$ and $L_e = 1 \text{ mm}$), and the outlet. Injected cells experience wall effect lift, F_{LW} , and shear-radiant lift, F_{LS} , in the focusing region, resulting in size-dependent lateral focusing and traveling velocity, U . When cells enter the electroporation chambers, cells with diameter larger than the threshold ($D_t \sim 15 \mu\text{m}$) are trapped in microscale vortices while smaller cells are flushed out of the device. (b) Average cell diameter and uniformity in size distribution of the trapped cells increased with the sample injection time. The average diameter of the captured metastatic breast cancer cells increased from $20 \pm 8.5 \mu\text{m}$ (coefficient variation (CV) of 40%) to $32 \pm 7.9 \mu\text{m}$ (CV of 25%) with increasing cell solution injection time. Image contrast is enhanced using ImageJ. Scale bar is $100 \mu\text{m}$.



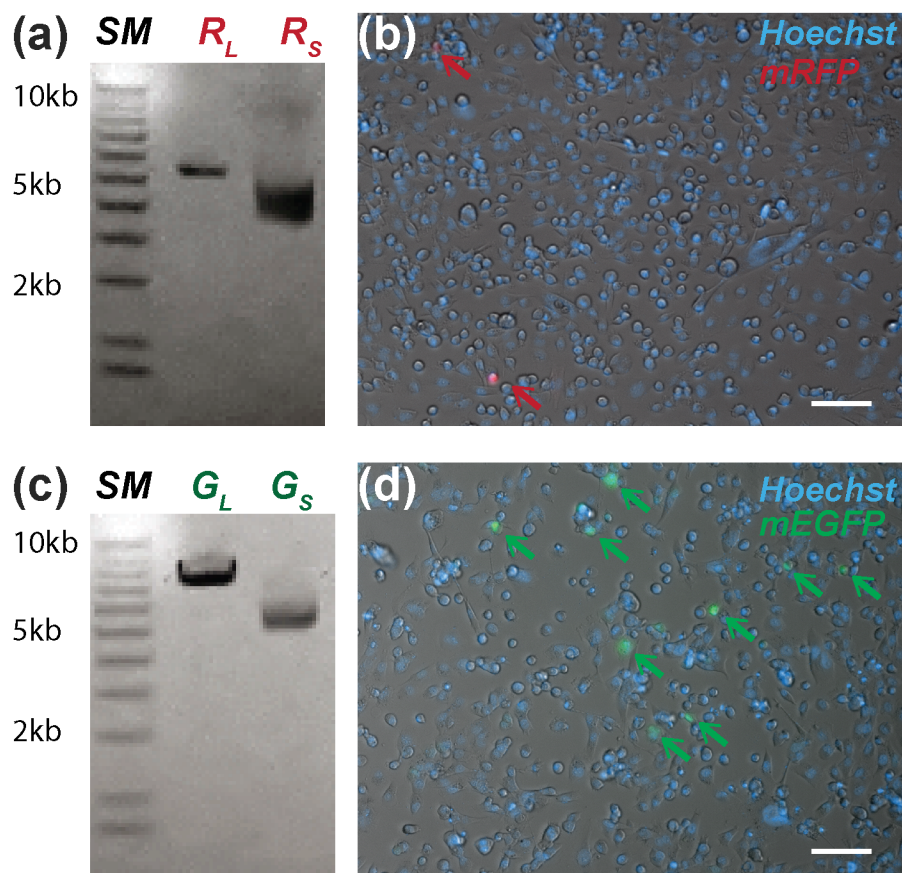
ESI Figure 2. Schematic of the computer-assisted pneumatic flow control system. Standard International Standard Organization (ISO) graphic symbols were used to better convey individual pneumatic components' functionality. Note that diagram is not to scale.



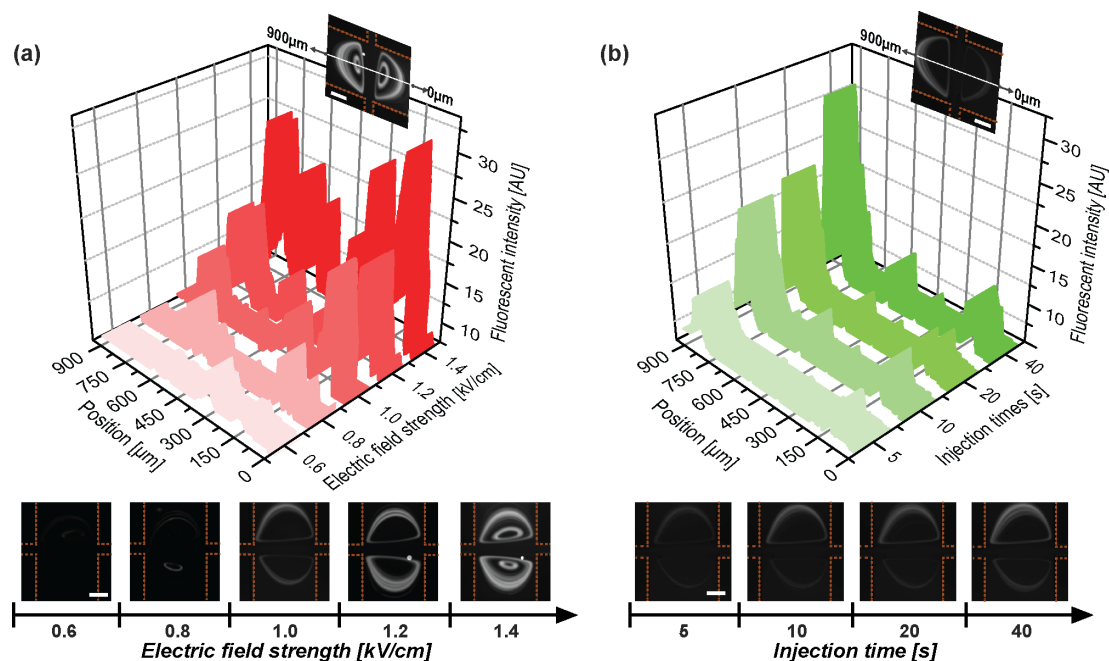
ESI Figure 3. Rapid solution exchange demonstration using a 1 μM FITC solution and a washing solution (DPBS). Time required to saturate the electroporation chambers with the desired molecular solution ($t = 8$ s) was found to be identical to that required to completely flush those chambers, suggesting a symmetric solution exchange scheme. Total injected amount of FITC molecules was 25 ng when saturation occurred. Image contrast is enhanced by adjusting look-up table (LUT). Scale bar is 100 μm .



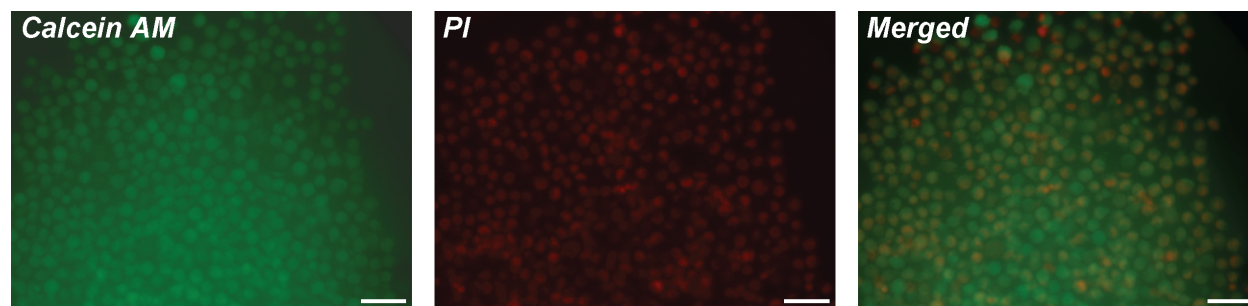
ESI Figure 4. Numerical simulations illustrate that the distribution of electric fields in the electroporation chamber is uniform and cell-trapping microscale vortices do not alter the distribution. Computed electric field strength distribution across the electroporation chamber is overlaid with (a) streamlines and (b) electric potential contours. Large gradient of the electric field was observed outside of orbits occupied by captured cells, thus it would not affect the electroporation performance adversely. Moreover, non-trapped cells would not be electroporated because no electric field gradient was observed in the straight inertial focusing channel. The simulation was conducted for 2D incompressible Navier-Stokes mode combined with the Electrocurrent mode using COMSOL[®] Multiphysics software (version 4.0). The fluid is considered to have the same properties as DPBS at room temperature (density, dynamic viscosity, and electric conductivity of 1000 kg/m³, 1.005 mPa·s, and 1.4 S/m, respectively). The pressure drop across the simulated region was set to be 20 psi since the electroporation chamber is located at 1.5 cm downstream from the inlet. No-slip boundary conditions were set on the channel walls and on the interfaces between electrodes and the fluid. Density, relative permittivity, and electric conductivity of platinum electrodes were set to 21,450 kg/m³, 7, and 9.43×10⁶ S/m, respectively. The applied voltage across the two electrodes was set to 70 V.



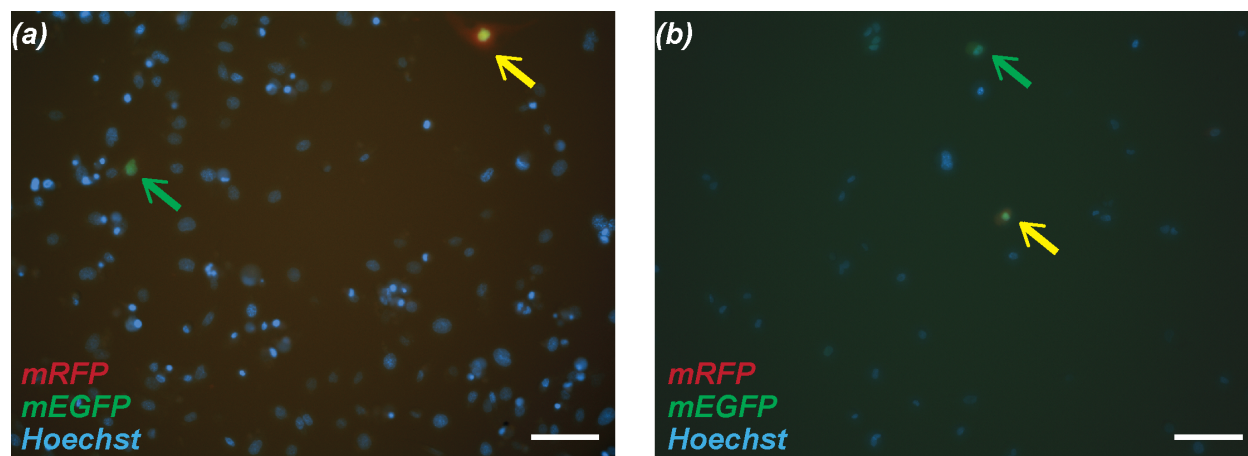
ESI Figure 5. The size and quality of (a and b) pcDNA3-mRFP (6118 bp, denoted as R) and (c and d) pQCXIP-NLS-Vx3-mEGFP (7919 bp, denoted as G) were verified using a gel electrophoresis and a chemical transfection technique. In order to determine the size of entire construction, mRFP and mEGFP plasmids were linearized by selecting BsmI and NheI-HF enzymes, respectively. Enzymes and reagents were purchased from New England Biolab[®] Inc. Subscription L and S indicate plasmids existing in full-length linear and supercoiled conformation, respectively. 1 kb DNA ladder (TrackIt[™], Invitrogen[™] USA) was used as the size marker (SM). Moreover, it was confirmed that MDA-MB-231 cells expressed (b) mRFP and (d) mEGFP once they were chemically transfected with pcDNA3-mRFP and pQCXIP-NLS-Vx3-mEGFP, respectively, using Lipofectamine[®] LTX with Plus[™] (Invitrogen) by following the protocol suggested by the manufacturer. Red and green arrows indicate cells transfected with mRFP and mEGFP genes, respectively. Transfected living cells were counterstained with Hoechst 33324 (NucBlue[®] Live ReadyProbes[™] Reagent, Life technologies[™]).



ESI Figure 6. The amount of the transferred PI molecules into K562 cells can be precisely controlled. Similar to MDA-MB-231 results, the amount of transferred PI molecules increased with increasing (a) electric field strength and (b) solution injection time. The electric field strength required to initiate molecular delivery was $E = 0.6$ kV/cm. All data were obtained from independently conducted experiments and their fluorescent intensities were quantified using the ImageJ software. LUT was adjusted to enhance contrast. Scale bars are 100 μm.



ESI Figure 7. Fluorescent microscopic images of K562 cells electroporated in the identical device under the static condition without vortex-assisted size-based pre-selection ($E = 1.5\text{ kV/cm}$). Molecules uptaken by electroporated cells were partially occupied. Living cells were stained with Calcein AM green prior to the electroporation and Propidium iodide (PI) was chosen as a molecule to be delivered. Note that PI uniformly stains non-viable cells, resulting in fluorescent signals overlapping with that of electroporated cells. Scale bars are $100\text{ }\mu\text{m}$.



ESI Figure 8. Representative fluorescent microscopic images of MDA-MB-231 cells obtained 48 hours after mEGFP and mRFP co-transfection using the conventional cuvette-type electroporation system at (a) $E = 0.4 \text{ kV/cm}$ and (b) $E = 0.8 \text{ kV/cm}$. While the viability of processed cells were strongly affected by increased electric field strength, apparent enhancement in the transfection efficiency has not been observed. Green and yellow arrows indicate cells transfected with mEGFP-only and both mEGFP and mRFP genes, respectively. Nuclei of living cells were stained with Hoechst 33342 (NucBlue® Live ReadyProbes™ Reagent, Life technologies™). Scale bars are $100 \mu\text{m}$.